Towards a Predictive Design Methodology of Composite Laminates and Patches: Physical Models of Environmental and Thermal Sensitive Failure Processes

PETER W. R. BEAUMONT

CUED/MAT-C/TR 244 (1998)

Third Report for EOARD

Towards a Predictive Design Methodology of Composite Laminates and Patches: Physical Models of Environmental and Thermal Sensitive Failure Processes

PETER W. R. BEAUMONT

Cambridge University Engineering Department
Trumpington Street, Cambridge CB2 1PQ, UK

Tel: (44) 01223 332 600
Fax: (44) 01223 332 662
e-mail: pwrb@eng.cam.ac.uk

This report was funded by the US Air Force and relates to a larger research program of the US Air Force Academy Colorado Springs, Colorado, USA
(Special Contract Program SPC 98-4004).

April, 1998.

Contents

Executive Summary

In two previous reports[1,2], a proposal was tabled for designing and certifying aerospace structures of composite laminate, and for repairing cracked aluminum structures using composite patches. In particular, it was based on sound fundamental understanding of the mechanisms by which damage accumulates in carbon fiber composites and structure across several orders of magnitude of size: fiber breakage and matrix cracking that lead progressively to ply failure; delamination and laminate cracking that lead to component fracture. Application of this approach to predictive design requires the necessary "know-how" and procedure for dealing with the identification of failure mechanisms from the micron to the metre level of size.

One method which is empirical in nature is to assess in sequence the effect of cyclic stress on the residual strength and lifetime of a test coupon, substructural element, component and finally large scale structure by a progression of experiments. This methodology is based on transferring empirical information and relating experimental data from one point on the size scale to another. Empirical methods, however, do have serious limitations and shortcomings.

The proposed way foward is to begin the design process at the constituent level with physical model-informed selection of fiber and it's surface treatment, matrix and it's processing condition, and choice of preferred architecture (geometry) of laminate construction. As the shift of information bothways along the size scale proceeds, the design process at each level of size evolves and includes the identification of the principal failure mechanisms, delamination, fiber fracture, and so on. A failure mechanism missed or not understood can have disastrous consequences on the life of the structure.

Making links or connections between our understanding of material and component behaviour relies critically on this knowledge of microscopic and macroscopic structural changes over the entire span of size and lifetime of the part. Hence, a technique for the evaluation of the conditions for growth (or no growth) of matrix cracks, delaminations and fiber fractures, for instance, is an essential tool in the determination of damage tolerance of composite material and structure. Numerical methods are generally available through the use of finite element

analysis and the crack closure integral technique based on fracture mechanics principles.

Whilst a fracture mechanics approach is not considered sufficiently mature at present to warrant a recommendation for general application to the certification of developmental composite hardware, nevertheless, this report considers the merits of fracture mechanics principles with respect to the important failure mechanism of fiber fracture, including fiber breaks precipitated by transverse ply matrix cracks. Individual cracks of these kinds can be treated using the principles of fracture mechanics; collectively, their effects on the properties of the material and structure can be quantified using relationships evolved from damage mechanics ideas[1,2].

In constructing a physical model, use is made of the tools of engineering and materials science: the equations and principles of mechanics, thermodynamics, kinetics, and so on. When the model is combined with experimental data of (say) fatigue strength, this approach leads to a design methodology having the power of prediction of lifetime which comes from an understanding of the relevant (meaning dominant) mechanism(s). At best, the model encapsulates the physical basis of the problem in mathematical form; it summaries what has been observed and predicts behaviour under conditions that have not been investigated.

The need to model the dominant mechanism(s) and to incorporate the model in the design process itself need only be pertinent in the first instance at the "microscopic" size level. It is important to consider, however, that the local tensile strength of the 0° ply within a damaged zone which ultimately determines laminate performance may be affected by:

(1) the presence of matrix-dominated ply cracks in the damage zone;

(2) the presence of a hostile environment which may lead to stress-corrosion cracking; and

(3) changes in temperature that set up thermal and residual stresses. For example, there is convincing evidence widely documented that the strength of glass fiber depends on the concentration of moisture in the atmosphere, and the degree of acidity or alkalinity. Also, that the shape of damage zones in carbon fiber-polymer composites is sensitive to temperature which affects matrix ductility, toughness, and so forth.

In reports 1 and 2, I considered matrix-dominated failure processes that can occur predominantly in carbon fiber-epoxy laminates (CFRP), essentially splitting and delamination. In this Third Report, I consider an additionl mechanism of failure that is dominant in glass fiber-epoxy laminates (GFRP) that of fiber fracture. In particular, this Third Report proposes a new physical-based micromechanical theory of stress-corrosion cracking in aligned continuous glass fiber-epoxy laminates.

This new theory is based on the premise that a crack initiates at a pre-existing surface flaw in glass fiber and extends by environmentally assisted slow crack growth. A prediction of macroscopic crack growth in the laminate by simultaneous matrix failure and fiber breakage is derived theoretically as a function of the crack tip stress intensity factor. Theoretical prediction which compares favourably with experimental measurement indicates that crack growth rate depends on the size of inherent surface flaw of glass fiber, the fiber-matrix interfacial bond strength, and matrix toughness.

Finally, for completeness, I have presented the essential ingredients of the splitting and delamination models[1,2] and equations for CFRP as an Appendix to this Report.

1. A Brief Overview of Design Philosophy

Traditionally, the process of design has involved specialised treatment of fatigue and corrosion fatigue phenomena. For metals this has meant obeying Miners rule and making good use of Goodman diagrams. For fatigue crack growth and stress-corrosion cracking, the Paris law of crack propagation has been applied with marked success. In sharp contrast, the treatment of similar phenomena for advanced composite structures is more complicated because of the complex formation of competing and interacting cracks in the material. (Metals generally fail by the growth of a single crack). Frequently, this has led to the composites industry experiencing hardware development problems due to design oversights that lead to a multitude of matrix cracks, splits and delaminations, and fiber fractures.

Furthermore, fundamental differences in the elastic properties and fracture toughness between fiber and matrix constituents prevent meaningful comparisons between material systems behaviour and damage tolerance although the nature of the fiber/matrix bond appears to play a significant role in the cracking and fracture processes. Consequently, the characteristics of damage accumulation from one material system to the next are not easily predictable due to this multiplicity and complexity of interacting cracks and competing failure modes.

An alternative innovative way foward is to begin the design process at the constituent level with physical model-informed selection of fiber and it's surface treatment, matrix and it's processing conditions, and architecture (geometry) of laminate construction[1, 2]. As the shift of information both ways along a *size scale* proceeds, from individual fiber to ply and from laminate to structure, the design process at each level of size has to include the identification of the principal failure mechanisms.

Where to begin the modelling process on the size scale depends upon the usefulness of that model and what it intends to accomplish. Making links or connections between our understanding of material and component behaviour at the various scale of sizes relies critically on information flow in both directions between higher and lower levels of *size*, and a working knowledge of microscopic and macroscopic structural changes over the entire span of size and lifetime of the component.

All to frequently, the effect of local details are identified very late in the design cycle and unfortunate experiences of this kind contribute in large part to early over optimism in the material's initial performance figures and design rating. Furthermore, any structural analysis performed at this stage has rarely been made in sufficient detail to adequately evaluate the effect of potential failure modes and margins-of-safety. Thus, those failure processes influenced by, for example, matrix properties which have a strong dependence on processing conditions and environment are susceptable to large statistical scatter and to cyclic loading effects.

Potential damage initiation sites include free edges, bolt holes, ply terminations, and, with respect to repair of structures, at a composite patch interface and patch itself. Hence, a technique for the evaluation of the conditions for growth (or no growth) of cracks is an essential tool for the determination of the damage tolerance of composite material and structure. Numerical methods are generally available through the use of finite element analysis and the crack closure integral technique based on fracture mechanics principles.

The application of fracture mechanics requires a significant analysis and test effort to evaluate "hot spots" within the structure and to generate the necessary fracture toughness data. Whilst a fracture mechanics approach is, therefore, not considered sufficiently mature at present to warrant a recommendation for general application to the certification of developmental composite hardware, nevertheless, I will consider the merits of fracture mechanics and damage mechanics principles.

2. A Brief Consideration of Fracture and Damage Mechanics

In most advanced composites, the earliest signs of damage comprises an array of matrix cracks in the individual transverse plies, often referred to as first ply failure. Following transverse ply cracking, delamination cracks accompanied by splits frequently form, including fiber breaks, precipitated by these transverse ply cracks[1, 2]. In reality, transverse ply cracks may already exist in the virgin material caused by a combination of thermal effects during processing and cooling and the mismatch of thermal expansion coefficients between adjacent layers of the laminate. Individual cracks of these kinds can be treated using the principles of fracture mechanics; collectively, their effects on the

properties of the material can be quantified using relationships based on damage mechanics ideas[1, 2].

Damage and fracture mechanics principles are based on quantitative relationships between microscopic and macrosopic parameters that attempt to "bridge" a gap that has opened up on the size scale between classical materials science that focuses, for example, on single fiber reinforcement models at the microstructural level, and structural engineering and hardware development at the one metre level and above. It is precisely at this gap that "design" normally changes hands from being a materials design issue to being a structural one for which neither group has taken responsibility.

In the stictest sense, "damage mechanics" refers to the *physical mechanisms* of multiple cracking by which damage forms and propagates in the material. The concept of continuum damage mechanics is a method of treating a "whole population of microscopic defects". In expressing that damage mechanics and fracture mechanics are complementary, one can consider that the final stage of damage mechanics is the initial stage of fracture mechanics where *single* crack growth of a major defective region or volume of material takes over.

Turning briefly at this particular point in the report to a related and also key aspect of design is the manner in which a material under stress reacts to the presence of stress concentrators such as holes or notches. Whilst a number of macroscopic empirical models[1, 2] offer the potential of working models to account for notch size effect they are considerably restricted in their application; for example, they do not provide insight into the mechanisms or causes of damage or the mechanics of ultimate failure. Neither do they predict a fracture stress for different intrinsic material variables or extrinsic (environmental and thermal) conditions other than those of the test; or provide insight into the connection between data at the laminate and microstructural levels; or even the reasoning behind the selection of fiber and matrix and process route in the first place. Such a design approach imposes a heavy burden of testing and data collection which is time-consuming and uneconomic in this current cost-conscious climate.

A logical way to progress might be to express the material and critical stress parameters of such correlations, if possible, as functions of the physical parameters that dictate failure. Some of these baseline

parameters can be described using the alternative approach to which I have drawn attention before[1, 2], that based on the physical modelling of actual failure processes and the effects these mechanisms have on localised stress in neighbouring load bearing plies. Interaction processes between mechanisms become extremely important since they determine the strength and fatigue lifetime of material and structure. They can best be understood if a physical model of each dominant mechanism is constructed[1, 2].

3. The Basis of a Model

A model is a gross simplification of the mechanism but containing the essential elements of which there are many types[1, 2]:

(1) *empirical models* which provide a mathematical description to a set of experimental data, with no power of prediction (an equation to fit the S-N curve of fracture stress versus load cycles to failure is a good example);

(2) *physical models* which have a predictive capacity since they are based on well-known physical processes (the mechanisms of delamination, splitting, and fiber fracture within a laminate are examples); and

(3) *static and dynamic models* which contain material properties that remain constant with time (the former) or show time or rate dependence (the latter). An example of the dynamic model is the rate-dependent behaviour of Kevlar fibers in epoxy due to a kinetic process of molecular unkinking in the fiber under monotonic or cyclic loading. Another example is the one described in this report, namely, stress-corrosion (or chemically assisted) cracking of glass fiber-epoxy laminates.

At the heart of the model, then, lies the physical mechanism(s) which can best be identified by direct observation using, for instance, optical or in-situ scanning electron microscopy. It is dangerous to assume a mechanism without evidence that it actually operates and is, or can be, dominant (meaning that it has more influence than other competing processes).

In constucting a model, use is made of the tools of engineering and materials science: the equations and principles of mechanics, thermodynamics, kinetics, and so on. And, of course, there is the menu of previously modelled problems of fracture (or damage) mechanics, of thermal stress and chemical (environmental) effects, and so forth. Many of the models have an empirical component which requires a more subtle approach or "fine tuning". An element of empiricism introduces unknown constants into the equation. Often, they simply multiply to produce only one, perhaps two, unknown constants. A calibration procedure is then required to set values on them; one experimental measurement for each constant. Fine tuning, then, simply means comparing the model's prediction to experimental measurements in a significant way, covering as wide a range of conditions as possible, fiber and matrix types, fiber lay-up, stress-state, number of fatigue cycles, temperature, environment, and so on.

The design of critical experiments is a vital element to this process. We can never get away from doing the pertinent experiment which is often pointed out and defined for us by the model itself. When the model is combined with experimental data of (say) fatigue strength, this approach leads to a design methodology having the power of prediction which comes from an understanding of the relevant (meaning dominant) mechanims.

At best, the model encapsulates the physical basis of the problem in mathematical form; it summaries what has been observed and predicts behaviour under conditions that have not been investigated. Caution is imperative when extrapolating the model; an unknown mechanism not previously encountered can have disastrous consequences. Microscopic models can provide insight into mechanisms of failure and *in parallel* with empirical methods they can be used to develop equations having the predictive power of physical modelling with the precision of curve-fitting. This approach is given respectability by having been assigned the name *"model-informed empiricism"* and it is this which has led to the development of the new branch of mechanics called *"damage mechanics"*.

The physical modelling approach, then, enables us to gain understanding of the origin of failure processes; to capture the material's response in an equation or code of design; to predict material behavior under conditions not easily simulated in the laboratory (for

example, extremely long duration fatigue tests); and to guide the optimisation of micro(macro)structure of the material for longevity and durability. The aim, then, of this approach is to establish a physical framework within which empirical descriptions of the behaviour of some (preferably all) of the experimental variables in composite design are embedded.

A word of warning: such procedures of developing a physical model (with empirical ingredients, as appropriate), may not work equally well for all systems. We are at a starting point. For comparison with the physical models of matrix-dominated failure processes in carbon fiber-epoxy laminates[1, 2], in this report I will address the development of a new micromechanical theory of stress-corrosion cracking of glass fiber-epoxy laminates based on the modelling of fiber fracture.

4. A Physical Model of Fiber Fracture Based on Direct Observation

Glass fiber-epoxy laminates can be weakened by the combined influence of stress and corrosive environment. For example, their susceptibility to stress-corrosion cracking in acidic environments has received wide attention[3-17]. Hogg and Hull[3], Noble et al.[8] and Price and Hull[9,12] have all observed stress-corrosion cracking of individual glass fibers in laminates using scanning electron microscopy. They observed that a *micron-sized* crack in glass fiber initiates at a surface flaw and propagates stably to begin with, followed by unstable (fast) propagation across the remainder of the fiber's diameter. The crack then extends further into the laminate as a *macroscopic* crack that can be seen using an optical microscope. In fracture mechanics terms, the relationship between macroscopic crack propagation rate, da/dt, and stress intensity factor, K_I, at the crack tip can be expressed by:

$$\frac{da}{dt} = AK_I^m \qquad (1)$$

where A and m are constants which depend on the material and environment.

For a slowly propagating macroscopic crack there is little or no fiber pull-out. The fracture planes of the fiber and matrix are coincidental. With increasing crack propagation rate, there is an increasing amount

of fiber-matrix interfacial debonding. As the macroscopic crack propagation rate increases this is accompanied by an increase in fiber-matrix interfacial debonding indicated by longer fiber pull-out.

The formation of matrix bridges in the crack wake are observed when tougher, more ductile matrices are used. Such mechanisms that act in the crack wake shield the tip of the crack from localised tensile stress.

In the next section, a theoretical relationship between the macroscopic crack propagation rate and the crack tip stress intensity factor is deduced. Comparison is made between theoretical prediction and experimental data which includes the effects of fiber-matrix debonding at the crack tip and matrix bridging in the crack wake.

5. A New Micromechanical Theory of Crack Propagation in GFRP (following Sekine and Beaumont, Cambridge (1998), unpublished)

Following the work of Wiederhorn and Bolz[19], the crack propagation rate, da/dt, in bulk glass due to stress-corrosion cracking is:

$$\frac{da}{dt} = v \exp\left(-\frac{E - \alpha K_I}{RT}\right) \qquad (2)$$

E is the activation energy of the chemically-activated process, K_I is the stress intensity factor, R is the gas constant, T is absolute temperature, and v and α are empirical constants.

On the surface of glass fiber are large numbers of flaws of variable size[10, 21]. It is reasonable to presume that a crack initiates at one of these pre-existing surface flaws and grows perpendicular to the fiber's length with time which leads to a time-dependence of fiber strength (Fig. 1).

Figure 2 shows a micrograph of a typical laminate fracture surface obtained by scanning electron microscopy. The fracture surface of each glass fiber is characterised by a smooth or "mirror" region which indicates slow cracking which is surrounded by a "hackle" region which indicates fast fracture. In the model, the shape of the slowly extending crack front is represented as a circular arc of radius r, where r is equal to

the fiber radius. The average crack propagation rate due to some stress-corrosion process can thus be written (from eqn (2)) as:

$$\left(\frac{1}{2r\theta}\right)\left(\frac{dX}{dt}\right) = \nu \exp\left(-\frac{E-\alpha K_I}{RT}\right) \qquad (3)$$

where X is the uncracked area of the fiber, θ is half the angle which is made by two fiber radii on the edges of the stress-corrosion crack, and t is time (Fig. 3). In eqn (3), the stress intensity factor K_I, should be interpreted as the average value of K_I along the entire length of the stress-corrosion crack tip. Since the stress intensity factor for the crack opening mode (designated by the subscript I) is constant, more or less, along the entire circular crack front, K_I can be represented by the stress intensity factor at the maximum depth of the stress-corrosion crack[22]:

$$K_I = \sigma F(\theta)\sqrt{2\pi r} \qquad (4)$$

where σ is the tensile stress acting on the fiber and $F(\theta)$ is written as

$$F(\theta) = \sqrt{1-\cos\theta}\left\{1.12-3.40(1-\cos\theta)+13.87(1-\cos\theta)^2-14.37(1-\cos\theta)^3\right\} \qquad (5)$$

For a model in which the aligned continuous glass fiber are distributed in a doubly periodic square array and perpendicular to the macroscopic stress-corrosion crack, the relationship between the tensile stress and the stress intensity factor for the crack opening mode is given by[17]:

$$\sigma = \beta K_I \qquad (6)$$

where:

$$\beta = \frac{1}{VV_f}\sqrt{\frac{2V_f^{1/2}}{r\pi^{3/2}}} \qquad (7)$$

Here V_f is the volume fraction of glass fiber and V is that fraction of plies of the laminate in which glass fiber are perpendicular to the macroscopic crack.

Furthermore, geometrical consideration of the area of the stress-corrosion crack (shown in Fig. 3) gives:

$$\frac{dX}{dt}=\frac{dY}{dt}=-4r^2\sin^2\theta\frac{d\theta}{dt} \tag{8}$$

where Y is the area of the stress-corrosion crack of the glass fiber.

Substituting eqn (8) into eqn (3) and combining eqns (4) and (6), we obtain:

$$dt=\frac{2r\sin^2\theta}{vk\quad\theta}\exp\left(-\frac{\alpha\beta F(\theta)\sqrt{2\pi r}}{RT}K_I\right)d\theta \tag{9}$$

where:

$$k=\exp\left(-\frac{E}{RT}\right) \tag{10}$$

By integrating eqn (9), the time required for the slow crack growth stage of failure of a single glass fiber by stress-corrosion cracking is given by:

$$t_F=\frac{2r}{vk}\int_{\theta_0}^{\theta_F}\frac{\sin^2\theta}{\theta}\exp\left(-\frac{\alpha\beta F(\theta)\sqrt{2\pi r}}{RT}K_I\right)d\theta \tag{11}$$

where θ_0 is half the angle made by two fiber radii on the edges of the pre-existing surface flaw and θ_F is the critical value at unstable (fast) fracture of the glass fiber.

Hogg and Hull[3], Aveston and Sillwood[7] pointed out that a feature of a slowly moving macroscopic stress-corrosion crack is the planar nature of the crack surfaces of the glass fiber and matrix with little fiber pull-out. The time of the brittle fracture (final) stage of glass fiber and surrounding matrix is much shorter than time t_F. It follows, therefore, that the macroscopic crack propagation rate, da/dt, is approximately given by:

$$\frac{da}{dt} = \frac{D}{t_F} \tag{12}$$

where D is the distance between neighbouring fibers in a doubly periodic square array of fiber (see Fig. 4), written as:

$$D = \sqrt{\frac{\pi}{V_f}} r \tag{13}$$

Substituting eqns (11) and (13) into eqn (12), we obtain:

$$\frac{da}{dt} = \frac{\sqrt{\pi} \nu k}{2\sqrt{V_f}} \left(\frac{1}{\int_{\theta_0}^{\theta_F} \frac{\sin^2 \theta}{\theta} \exp\left(-\frac{\alpha\beta F(\theta)\sqrt{2\pi r}}{RT} K_I \right) d\theta} \right) \tag{14}$$

At this point are introduced the following quantities:

$$\xi = \frac{\sqrt{\pi}}{2} \left(\frac{\nu k}{\sqrt{V_f}} \right), \quad \mu = \frac{\alpha\beta\sqrt{2\pi r}}{RT} \tag{15}$$

so that eqn (14) can be rewritten as:

$$\frac{da}{dt} = \left(\frac{\xi}{\int_{\theta_0}^{\theta_F} \frac{\sin^2 \theta}{\theta} \exp(-\mu K_I F(\theta) d\theta} \right) \tag{16}$$

Consider the result of integrating the denominator in the above equation. Choosing sensible values of α = 0.11 ~ 0.216 $m^{5/2}$ / mol [21], V_f = 0.40~0.57, V = 0.5 for a cross-ply laminate and V = 1.0 for a

unidirectional laminate, R = 8.31 J/(mol.K) and T = 298 K, the integration gives a value of μ estimated within the range:

$$\mu = 102 \sim 521 \text{ (MP m}^{1/2})^{-1} \qquad (17)$$

Generally speaking, the range of experimentally observed stress intensity factor K_I at the crack tip is between 2 and 15 MPa.m$^{1/2}$. It follows that the integrand of the denominator of eqn (16) tends to zero, except for very small values of θ. Thus, the denominator, which is denoted by I, can be written approximately as:

$$I = \int_{\theta_0}^{\theta_F} \sin\theta \exp\left(-1.12\mu K_I \sqrt{1-\cos\theta}\right) d\theta \qquad (18)$$

Performing the integration:

$$I = -4\left[\left(\frac{1}{1.58\mu K_I}\right)\left(\frac{1}{1.58\mu K_I}+\theta\right)\exp\left(-1.58\mu\theta K_I\right)\right]_{\theta=\theta_0}^{\theta=\theta_F} \qquad (19)$$

$$\text{where } \theta_0 = \sin\frac{\theta_0}{2}, \quad \theta_F = \sin\frac{\theta_F}{2} \qquad (20)$$

Since the angle θ_0 is small and much smaller than θ_F, it follows that:

$$\exp\left(-1.58\mu\theta_0 K_I\right) \rangle\rangle \exp\left(-1.58\mu\theta_F K_I\right) \qquad (21)$$

Eqn (19), therefore, reduces to:

$$I = \left[\left(\frac{4}{1.58\mu K_I}\right)\left(\frac{1}{1.58\mu K_I}+\frac{\theta_0}{2}\right)\exp\left(-0.79\mu\theta_0 K_I\right)\right] \qquad (22)$$

Substituting eqn (22) into the denominator of eqn (16), the macroscopic crack propagation rate, da/dt, can be written in the form:

$$\frac{da}{dt} = 1.25\xi\mu^2 K_I\left(\frac{1}{2+1.58\mu\theta_0 K_I}\right)\exp\left(0.79\mu\theta_0 K_I\right) \qquad (23)$$

This equation indicates that the macroscopic crack propagation rate is independent of fibre radius r because μ is independent of r. Furthermore, the macroscopic crack propagation rate is independent of the fracture toughness of glass fiber.

6. Results and Discussion

6.1 *Verification by experiment*

There is experimental data in the literature[16, 17] on a cross-ply laminate of E-glass fiber (52.4% by vol.) in a diglycidyl ether of bisphenol-A-type epoxy resin matrix. The laminate consists of 44 plies with an individual ply thickness of about 0.14mm and a stacking sequence of $(0°/90°)_{11s}$. Compact tension specimens with side grooves were machined from the laminate. The apparent fracture toughness K_C of the laminate was 18.2 MPa.m$^{1/2}$ measured in air at room temperature.

Stress-corrosion crack propagation tests were carried out in 0.5N HCl at 298K under constant load. During tests, crack "mouth" displacement was measured at intervals using a linear variable displacement transducer. The macroscopic crack length was estimated from crack mouth displacement by means of a finite element method. Estimates of macroscopic crack propagation rate were obtained by averaging the derivative of the macroscopic crack propagation length with respect to time over an interval of between 4 and 24 hours.

Figure 5 shows a logarithmic plot of the experimental values of macroscopic crack propagation rate versus the crack tip stress intensity factor. The figure reveals a linear log (da/dt) - log K_I relationship over a an order of magnitude range of da/dt. Comparison between experiment and theory can be made by setting values of ξ and μ, and θ_0 and calculating the macroscopic crack propagation rate, da/dt, for the particular stress intensity factor K_I using eqn (23). Following reference[16] where a best fit method was used, we take ξ, and μ and θ_0 as $\xi = 5.01 \times 10^{-15}$ m.s^{-1}, $\mu = 228$ (MPa.m$^{1/2}$)$^{-1}$ and $\theta_0 = 0.215°$. The prediction of macroscopic crack propagation rate is shown by the solid line in Fig. 5, and is in good agreement with experimental

measurement. This gives confidence in the physical interpretation of macroscopic crack propagation in aligned continuous GFRP laminates.

6.2 *Macroscopic crack propagation rate for the limiting values of* θ_0

The size of a pre-existing surface flaw on glass fiber affects significantly the macroscopic crack propagation rate of the laminate. Eqn (23) indicates that the macroscopic crack propagation rate increases monotonically with the angle θ_0 of the pre-existing surface flaw of the glass fiber.

First, consider the case where $\theta_0 = 0$, where the glass fibers are free of surface flaws. In this case, eqn (23) reduces simply to:

$$\frac{da}{dt} = 0.625\xi\mu^2 K_I^2 \tag{24}$$

Substitution of eqns (7) and (15) into eqn (24) yields:

$$\frac{da}{dt} = \frac{1.25\alpha^2 \nu k}{V^2 V_f^2 R^2 T^2} K_I^2 \tag{25}$$

Equation (25) indicates the minimum macroscopic crack propagation rate of an aligned continuous GFRP laminate with respect to θ_0, and demonstrates that the variation of da/dt with K_I obeys a simple power law having a power of 2. This value is independent of laminate geometry and acidic environment.

Table 1 shows the values of power given in reported studies[7, 9, 11, 12, 15]. All the values of power are larger than 2. It appears from these experimental results that the lowest value of power is likely to be 2.

Meanwhile, let us consider the case of large values of θ_0 and consider Bartenev's[20] view that the depth of a pre-existing surface flaw of fine commercial glass fiber is no greater than 0.01 microns. In this case, the angle θ_0 would be roughly 2.5° (or 4.36×10^{-2} rad). When θ_0 is large

and comparable with 2.5°, $\mu\theta_0 K_I$ exceeds unity. Eqn (23) then reduces to:

$$\frac{da}{dt} = \frac{0.79\xi\mu}{\theta_0} K_I \exp\left(0.79\mu\theta_0 K_I\right) \qquad (26)$$

In this case, the macroscopic crack propagation rate, da/dt, is faster than would be expected using the simple power law. The macroscopic crack propagation rate at high values of stress intensity factor is discussed below.

6.3 *Effect of fibre-matrix interfacial debonding on macroscopic crack propagation rate*

For a slowly propagating macroscopic crack there is little or no fiber pull-out. In spite of possible environmental degradation of the fiber-matrix interface, the fracture planes of the fiber and matrix are coincidental. In contrast, with increasing crack propagation rate, the crack path is more tortuous due to an increasing amount of fiber-matrix interfacial debonding. The greater the extent of fiber-matrix debonding, the greater the likelihood of exposure of a larger surface flaw in glass to environmental attack.

Figure 6 shows the relationship between the macroscopic crack propagation rate and the stress intensity factor for θ_0 = 0.2°, 0.3° and 0.4°. The values of ξ and μ are held constant as before. A feature of crack propagation coexisting with fiber-matrix interfacial debonding is schematically illustrated by the broken line in the figure. The macroscopic crack propagation rate increases when the stress intensity factor increases and fiber-matrix interfacial debonding occurs indicated by longer fiber pull-out.

6.4 *Effect of matrix toughness on macroscopic crack propagation rate*

The effect of matrix toughness on stress-corrosion cracking was studied by Price and Hull[12] using the scanning electron microscope. They observed the formation of matrix bridges in the crack wake when tougher, more ductile matrices were used. Such mechanisms that act in the crack wake shield the tip of the crack from

local stress. Fig. 7 shows bridging over a crack of width l. Now the localsed stress in the matrix at the crack tip is of the order of it's yield stress. Consequently, when matrix bridging occurs, the reduced crack tip stress intensity factor is given by[23]:

$$K_I - 4\sigma_{ym}\sqrt{\frac{l}{2\pi}} \tag{27}$$

By substituting eqn (27) for K_I into eqn (23), the macroscopic crack propagation rate in terms of K_I is given by:

$$\frac{da}{dt} = 1.25\xi\mu^2\left(K_I - 4\sigma_{ym}\sqrt{\frac{l}{2\pi}}\right)^2 x\left\{2+1.58\mu\theta_0\left(\left(K_I - 4\sigma_{ym}\sqrt{\frac{l}{2\pi}}\right)\right)\right\}^{-1} x\exp\left\{0.79\mu\theta_0\left(\left(K_I - 4\sigma_{ym}\sqrt{\frac{l}{2\pi}}\right)\right)\right\} \tag{28}$$

The numerical results of eqn (28) are presented graphically for l = 0, 1, 2 and 3 microns, σ_{ym} = 80MPa, and the values of ξ, μ, and θ_0 were the same as those values used previously (Fig. 8). The macroscopic crack propagation rate decreases as the size of the matrix bridge increases. This bridging effect is more pronounced at lower values of K_I and is schematically shown by the broken line in Fig. 8.

7. Conclusions

A physically-based micromechanical theory of crack propagation due to stress-corrosion cracking in aligned continuous GFRP laminates has been established. Good agreement between experiment and theory give confidence in our model. When the relationship is expressed for the limiting case where the glass fibers are free of pre-existing surface flaws, the relationship is represented by the simple power law with the value of power of 2. The effects of fiber-

matrix interfacial debonding and matrix toughness on the macroscopic crack propagation rate are taken into account by the theory.

8. Implications and Final Remarks

In the example of predicting the behavior of a laminate, it might be argued that it would be equally cost-effective to simply perform the mechanical tests under conditions that span the predictive range of the model. However, if the objective is to design for longevity and durability, then the balance is shifted in favour of physical modelling. It is in this area that the application of the model is most powerful.

The economic advantage of reducing the high cost of vast experimental programs in assorted environments and stress-states having durations of many thousands of hours is potentially huge. In addition, physical modelling provides the means to assess the relative severity of different loading regimes, e.g., constant amplitude vs. variable amplitude spectra, frequency effects and R-ratio effects as well as load/environment interactions, as described in this report. This capability is important in the design of experimental test programs that ensure critical loading regimes are examined.

Furthermore, even though modelling of this kind may be of limited benefit for predicting, for example, the notched fracture stress in quasi-static loading (the effect of lay-up, hole size, environment, and so forth), these models are valuable inasmuch as they draw attention to the precise features of the failure process that have wider significance and implications.

Certain capabilities are missing. It does have it's limitations; in particular, it lacks the ability to link the observed damage growth of splits, transverse ply cracks, delaminations, fiber fractures growing in a coupled manner to models for the growth of individual damage modes growing in isolation.

This modelling approach, as currently presented, does not have the capability of coping with variations in damage mode interactions from system to system. Thus, whilst modelling matrix-dominated failure processes works well for carbon fiber composites where the *in situ* strength of the 0° ply in the fatigue-damaged laminate is not

significantly different from the strength of undamaged unidirectional material, by contrast, an alternative model is required for the failure of glass fiber composites that reflects an input for strength degradation (this Report).

There is scope to integrate this modelling approach with the large experimental programs that are currently employed to design fracture critical components and structures. However, this step has yet to be made. This last point requires elaboration. Modelling a particular problem is only a sub-element of the overall design process. I believe that the philosophy behind the physical modelling approach has wider applicability. In particular, the foundation of physical modelling could be applied to other problems. One important area is based on composite patch repair of metallic structures.

Modelling the mechanisms of damage and relating them to experimental data and empirical correlations that are currently employed in design provides a first attempt at achieving a predictive capability in design, particularly with regard to issues of strength, durability and longevity. It has the potential to provide a cost-effective alternative to the present largely empirical approach which takes an excessively long time and is expensive. Even the exercise of observing the operative damage mechanisms and calibrating the model for quasi-static loading provides useful physical insight which is currently not available to the structural design engineer or materials technologist.

However, the development of this alternative design methodology should be an evolutionary process with short and long term benefits. In the short term current mechanistic models can be used to bound problems, identify critical material properties, and map likely failure modes. This will lead to improved test programs which concentrate on critical issues and failure modes investigated at the important size scale(s).

Since the models must be based on experimentally-observed phenomena, experimental data will help to improve and "fine tune" them and there will thus be a synergistic effect. In the longer term, improved modelling will allow designers to begin the design process with an intelligent choice of constituent materials and interfaces and then to proceed with the prediction of performance and failure at the

various size scale, i.e., fiber, ply, laminate, structural component, full scale structure.

Existing design methodology at the higher structural size scales will thus be supported and justified by fundamental understanding at lower size scales. Added benefits of this approach include more options being available to the designer, a reduced need for extensive and costly testing and more efficient and shorter design iteration cycles. This will lead to more versatile, more cost-effective, and more efficient composite products, and thus help to fulfil the promise of composite materials.

Finally, the key steps that underpin the modelling described here are: mechanical testing, characterization of mechanisms by observation and modelling of these physical mechanisms to predict structural response. If these steps were routinely followed as part of the design process it would potentially have a profound effect on the overall cost-effectiveness of that process.

Acknowledgements

I would like to record my gratitude to Major Rob Fredell of The US Air Force Academy, Colorado Springs for supporting different aspects of this work as it relates to the failure of composite laminates and bonded patches.

References

1. Beaumont, P.W.R., Predictive Design and Certification Procedures: Modelling Fracture Stress, Fatigue Strength and Life-time of Composites and Structures. CUED/C-MATS/TR 241. First Report for EOARD (Special Contract Program SPC 98-4004), (January, 1998). Cambridge University Engineering Department, Cambridge, UK.
2. Beaumont, P.W.R., Towards a Predictive Design Methodology of Composite Laminate Patches Based on Physical Modelling of Failure Processes. Second Report for EOARD (Special Contract Program SPC 98-4004), February, 1998. Cambridge University Engineering Department, Cambridge, UK.
3. Hogg. P. J & Hull, D., Micromechanisms of crack growth in composite materials under corrosive environments. J. Mater. Sci., 14 (1980) pp. 441-9.
4. Carswell, W. S. & Roberts, R. C., Environmental fatigue stress failure mechanism for glass fibre mat reinforced polyester. Composites, (1980) pp. 95-9.
5. Hogg, P. J., Hull, D. & Spencer, B., Stress and strain corrosion of glass-reinforced plastics. Composites, 12 (1981) pp. 166-72.
6. Friedrich, K., Stress corrosion crack propagation in glass fibre reinforced/thermoplastic PET. J. Mater. Sci., 16 (1981) pp. 3292-302.
7. Aveston, J. & Sillwood, J. M., Long-term strength of glass-reinforced plastics in dilute sulphuric acid. J. Mater. Sci., 17 (1982) pp. 3491-8.
8. Noble, B., Harris, S. J. & Owen, M. J., Stress corrosion cracking of GRP pultruded rods in acid environments. J. Mater. Sci., 18 (1983) pp. 1244-54.
9. Price, J. N. & Hull, D., Propagation of stress corrosion cracks in aligned glass fibre composite materials. J. Mater. Sci., 18 (1983) pp. 2798-810
10. Lhymn, C. & Schultz, J. M., Chemically-assisted fracture of thermoplastic PET reinforced with short E-glass fibre. J. Mater. Sci., 18 (1983) pp. 2923-38.
11. Hsu, P.-L., Yau, S.-S & Chou, T.-W., Stress-corrosion cracking and its propagation in aligned short-fibre composites. J. Mater. Sci., 21 (1986) pp. 3703-9.
12. Price, J. N. & Hull, D., Effect of matrix toughness on crack propagation during stress corrosion of glass reinforced composites. Comp. Sci. Technol., 28 (1987) pp. 193-210.

13. Kumosa, M., Hull, D. & Price, J. N., Acoustic emission from stress corrosion cracks in aligned GRP. J. Mater. Sci., 22 (1987) pp. 331-6.
14. Miyanaga, T. & Sekine, H., Micromechanics study of crack propagation rate in glass fiber reinforced plastics under acid environments. J. Soc. Mater. Sci., Jpn., 39 (1990) pp. 737-41
15. Sekine, H. & Miyanaga, T., A micromechanics study of crack propagation rate by stress corrosion in glass fiber reinforced plastics in consideration of pre-existing microcracks on the surface of fibers. J. Soc. Mater. Sci., Jpn., 39 (1990) pp. 1545-8.
16. Sekine, H. & Miyanaga, T., A micromechanics study of the effects of concentration and temperature on the propagation rate of stress corrosion crack in cross ply glass/epoxy laminates under acid environments. J. Soc. Mater. Sci., Jpn., 41 (1992) pp. 1132-5.
17. Sekine, H., Micromechanics study of the propagation rate of a stress corrosion crack in cross ply glass/epoxy laminates under acid environments. Proc. 8th Int. Conf: Comp. Mater., 1991, pp. 27 K-1-10.
18. Sekine, H., Hu, N. & Fukunaga, H., Direct numerical simulation of the extension of stress-corrosion cracks in glass fibers embedded in laminates in acid environments. Comp. Sci. Technol., 53 (1995) pp. 317-323.
19. Wiederhorn, S. M. & Bolz, L. H., Stress corrosion and static fatigue of glass. J. Am. Ceram. Soc., 53 (1970) pp. 543-8.
20. Bartenev, G. M., Constitution and strength of glass fibers. Int. J. Fract. Mech., 5 (1969) pp. 179-86.
21. Piggott, M. R. & Yokom, J. C., The weakening of silica fibres by heat treatment. Glass Technol., 2 (1968) pp. 172-5.
22. Kiuchi, A., Aoki, M., Kobayashi, M. & Ikeda, K., Evaluation of brittle fracture strength of surface notched round bar. J. Iron Steel. Inst. Japan, 68 (1982) pp. 1830-8.
23. Sih, G. C., Handbook of Stress-Intensity Factors. Lehigh Univ., 1973.

Fig. 1 Model of crack propagation in glass fibers

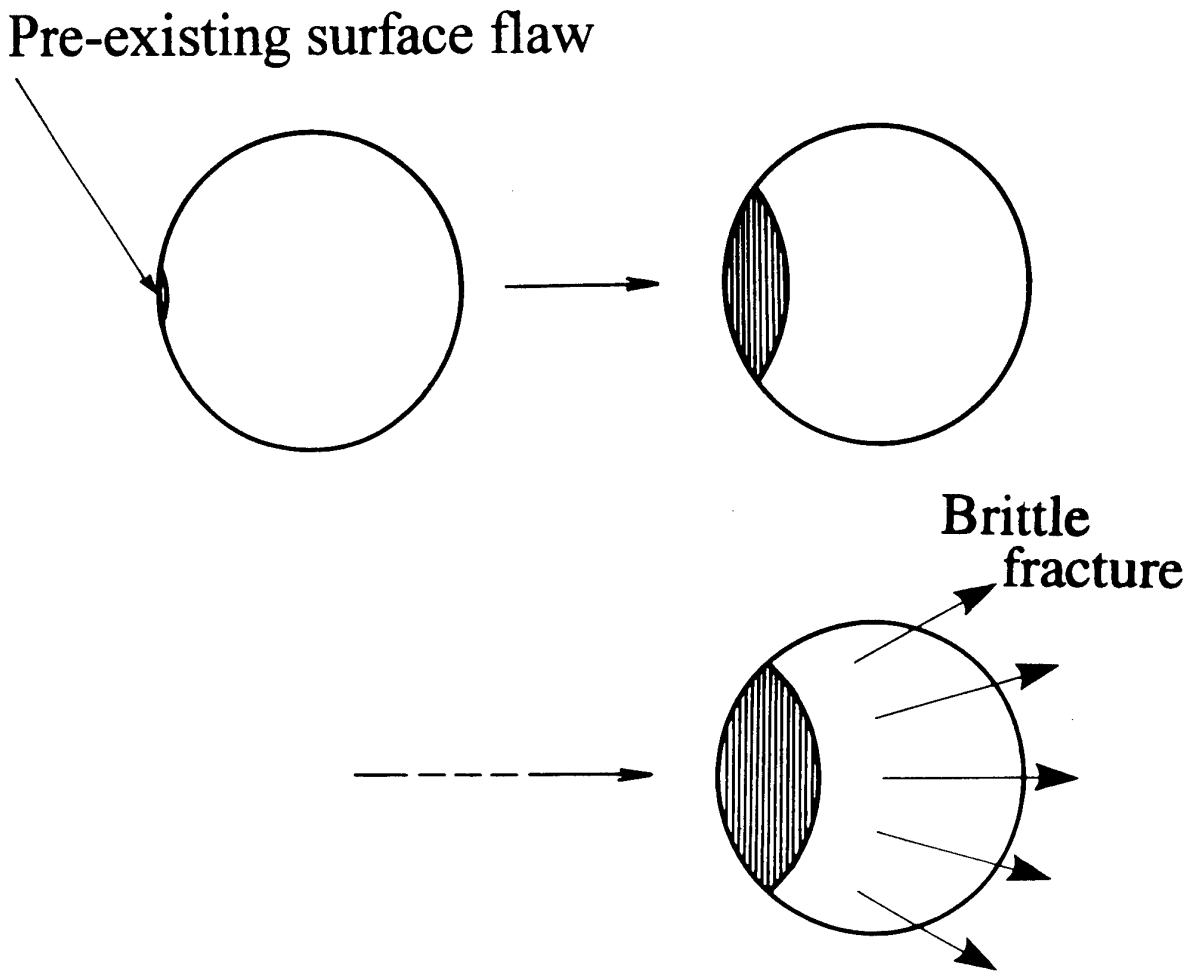

Fig. 2 Scanning electron micrograph of fracture surfaces of glass fibers

Fig. 3 Shape of stress-corrosion crack in glass fibers

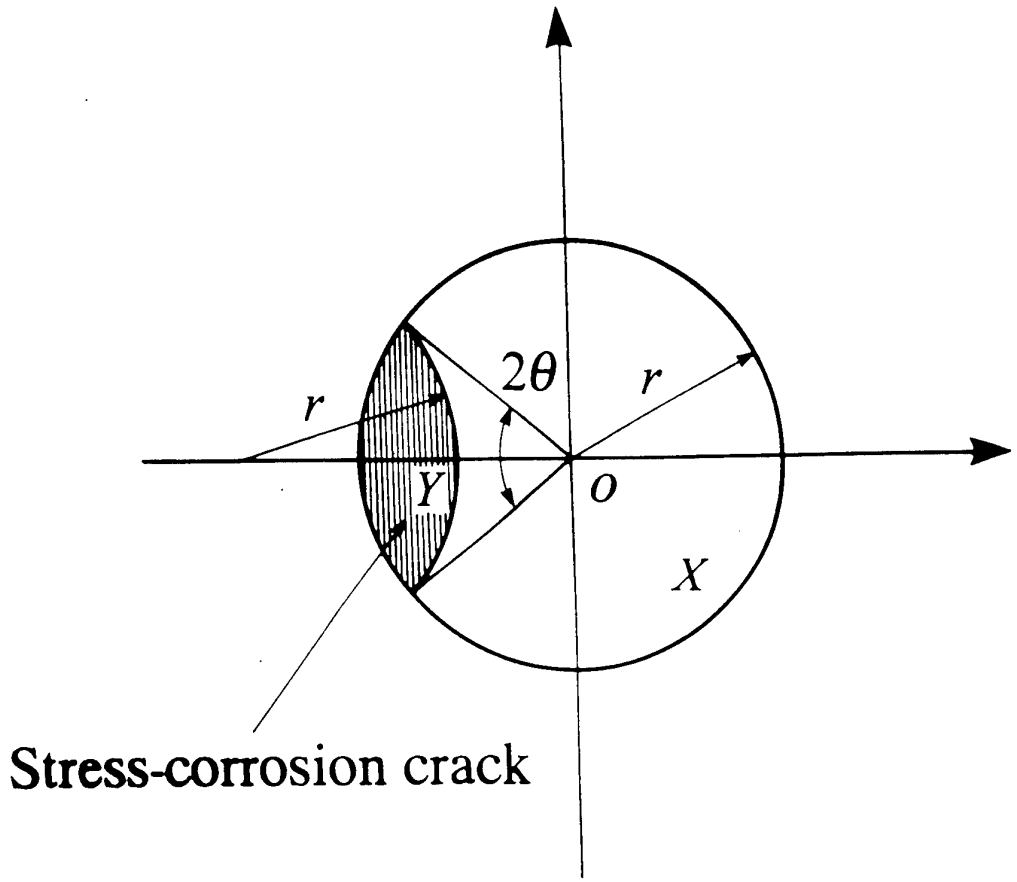

Fig. 4 Glass fibers distributed in a doubly periodic square array.

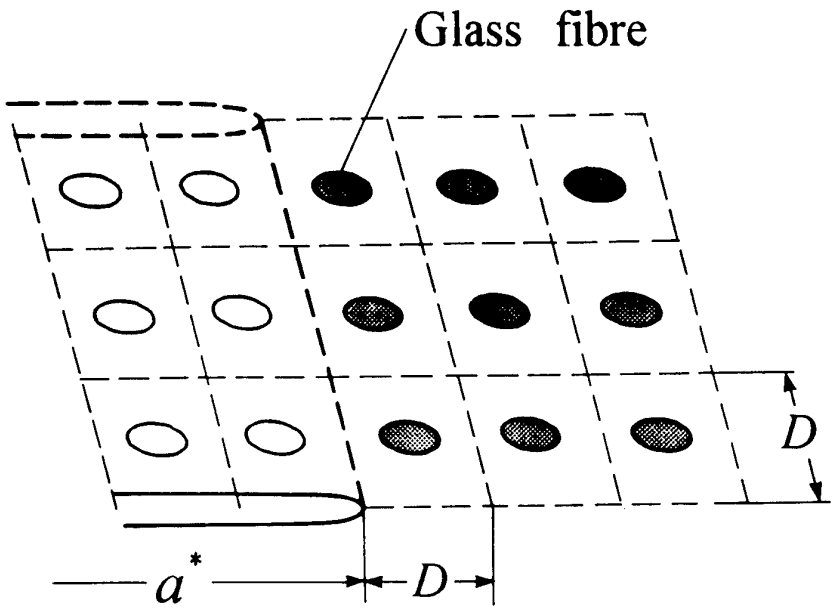

Fig. 5 Macroscopic crack propagation rate versus the stress intensity factor at the macroscopic crack tip.

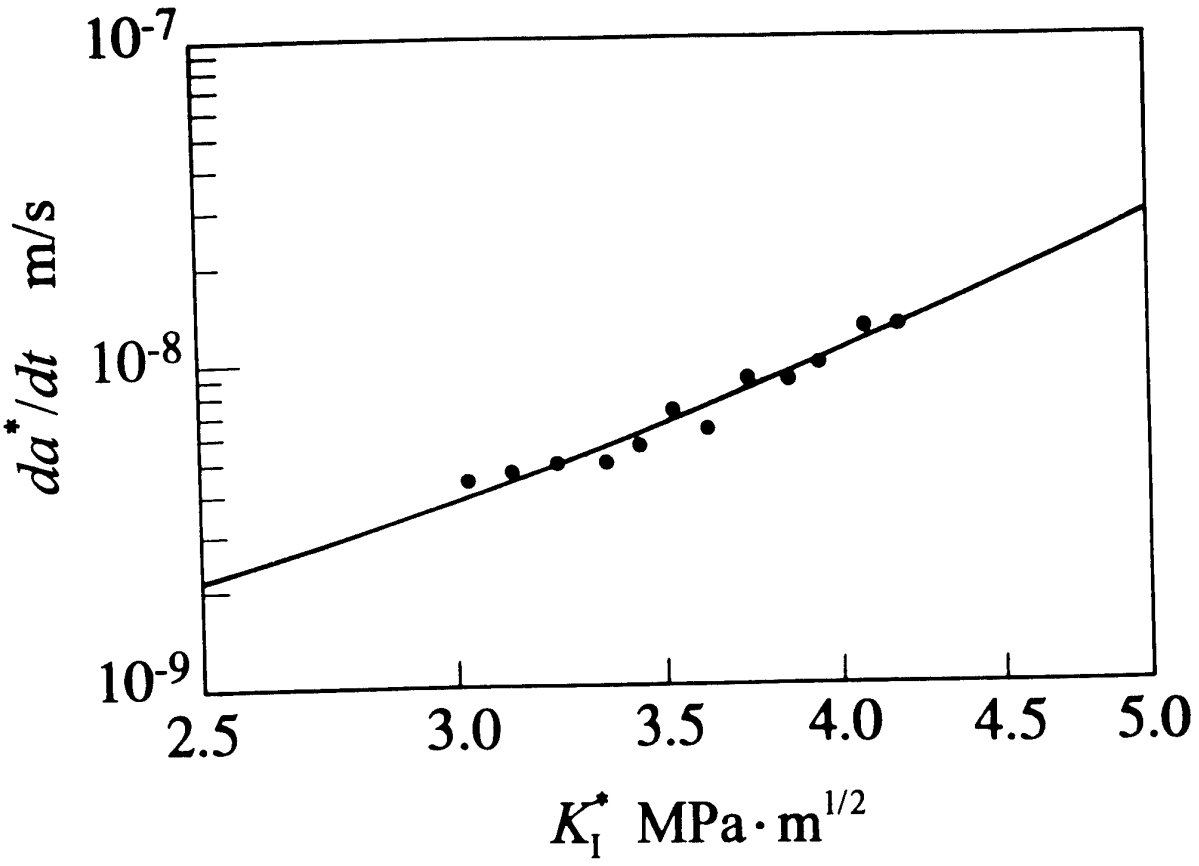

Fig. 6 Macroscopic crack propagation rate in a state of fiber-matrix interface debonding.

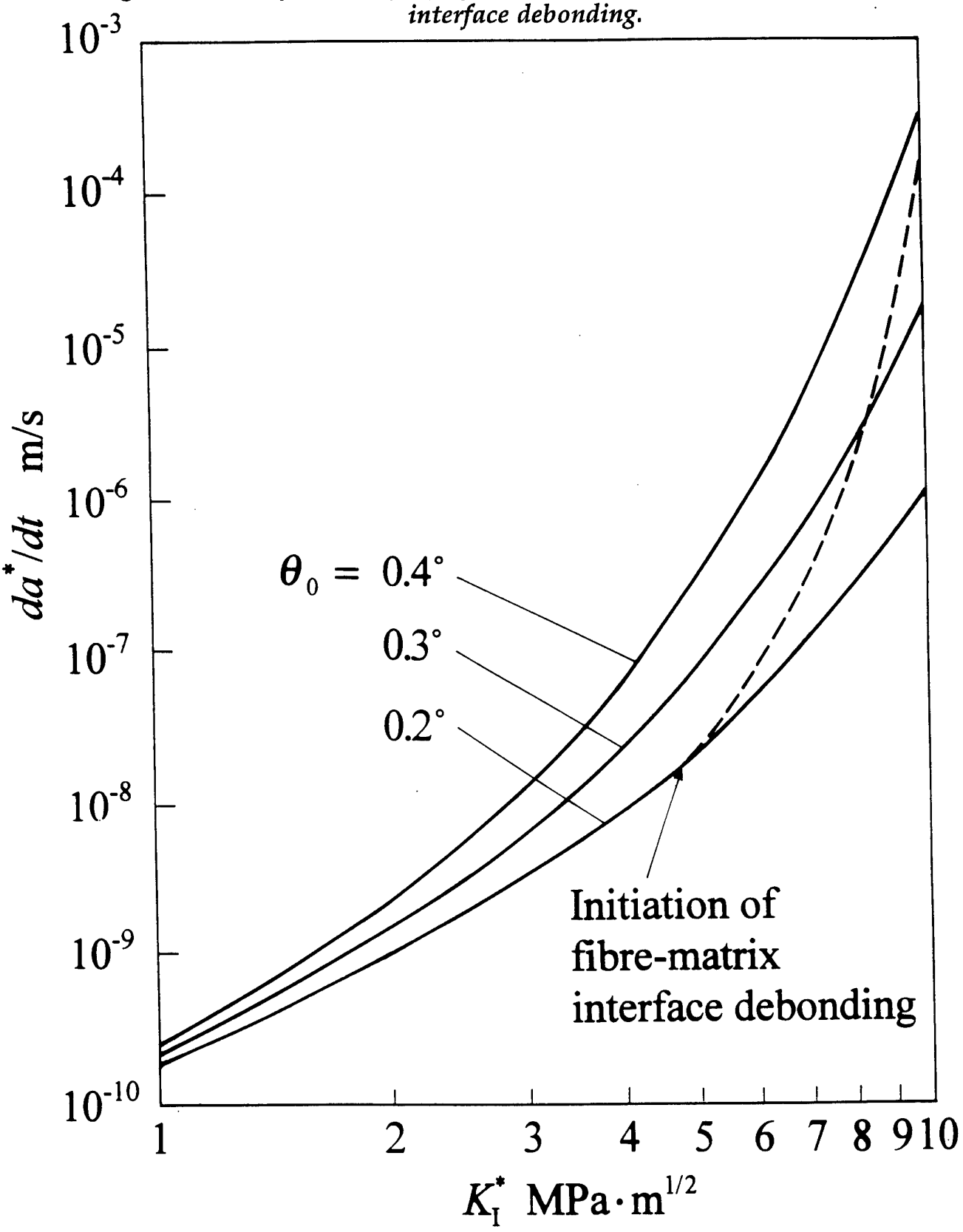

Fig. 7 Matrix bridging at the crack front of a macroscopic stress-corrosion crack.

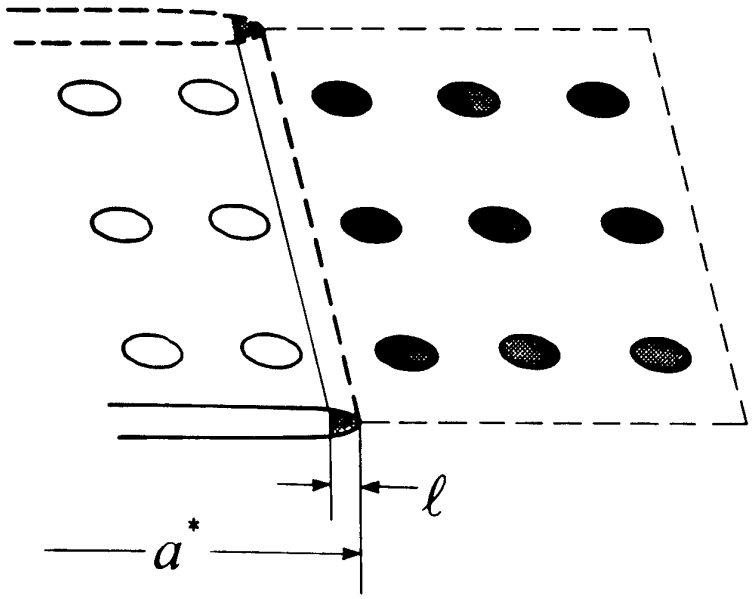

Fig. 8 Macroscopic crack propagation rate in a state of matrix bridging.

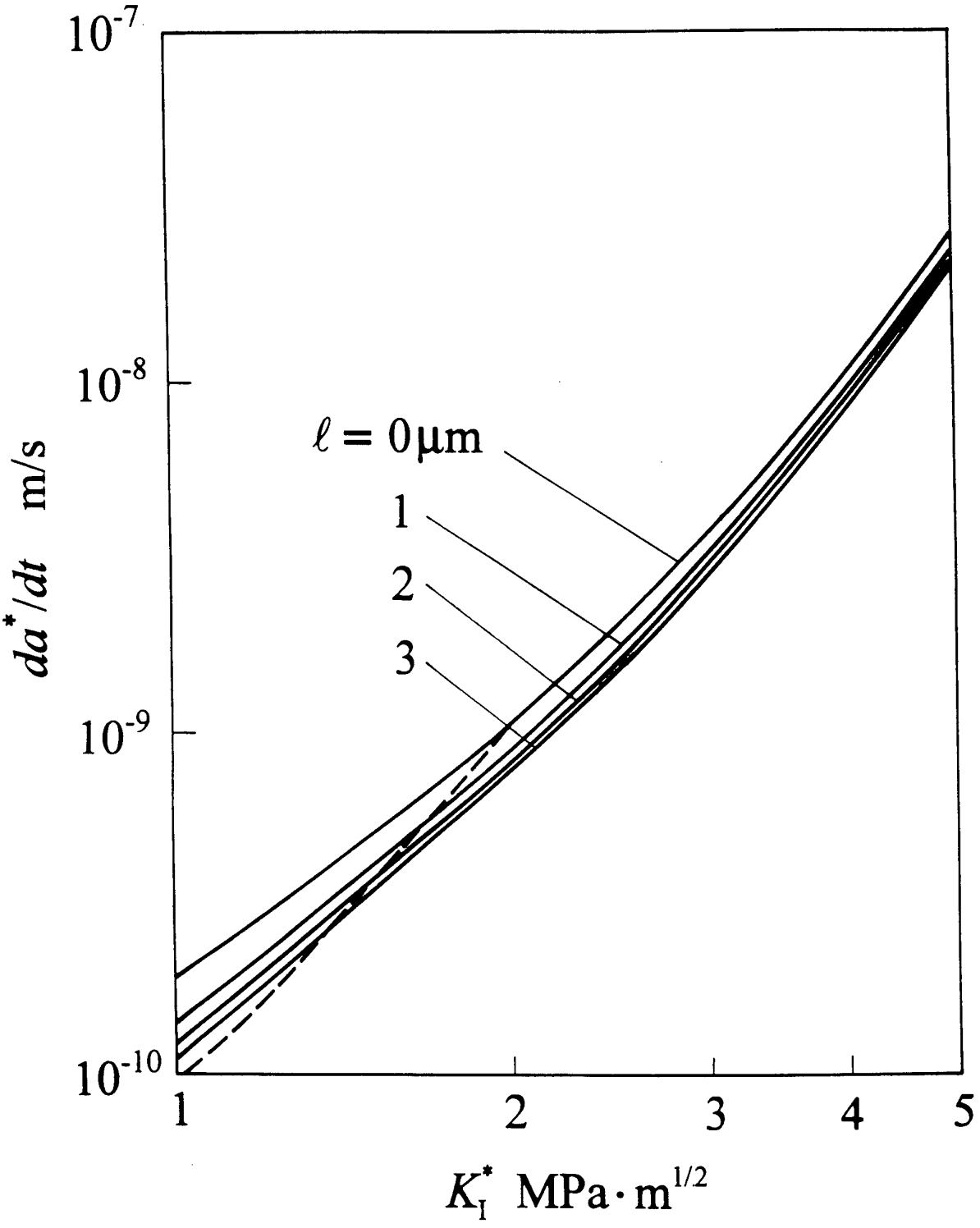

Table 1 Values of power in a simple power law equation.

Lay-up	Environment	Value of Power	Ref
Unidirectional E-glass/polyester	1.0N H_2SO_4	3.1	5
Unidirectional E-glass/polyester	0.6N HCl	3.8	7
Cross-ply short E-glass/epoxy	1.0N H_2SO_4	6.3	9
Unidirectional E-glass/polyester	0.6N HCl	3.6	10
Cross-ply short E-glass/epoxy	0.5N HCl	3.6	15

Appendix: Thermal and Residual Stress Effects on Damage Accumulation in Carbon Fiber-Epoxy; Modelling the Failure Processes

Damage Observed Around Notches

An X-ray image of a typical $(90/0)_s$ notched tensile specimen of carbon fibre in epoxy loaded in tension indicates three forms of matrix crack emanating from within the notch tip damage zone[1,2]:

(1) *splitting* in the 0° plies;
(2) *delamination* zones at 90/0 interfaces whose size is related to split length; and
(3) *transverse ply cracking* in the 90° plies.

A concentration of fibre breaks in the 0° plies occurs at the intersection of a split and a transverse ply crack.

In a monotonic tensile test or in a cyclic loading experiment, the shape of the damage zone remains unaffected; it simply grows in size in a self-similar manner, with a characteristic triangular-shaped delamination zone at the (90/0) interfaces. At the tip of the split, the delamination angle, (between about 1° and 7°) depends on ply thickness, on matrix toughness, temperature, moisture content. Essentially, the damage pattern at the notch tip can be characterised by the delamination angle and split length. This ignores the transverse ply cracks in the matrix which are important but they can play a secondary role.

Modelling Damage in Monotonic Loading

The change in potential energy of a system as a crack grows is given by the change in strain energy less the work done by the applied loads. For an infinitesimal amount of crack growth, the energy released under fixed load or fixed displacement conditions is equal to:

$$\delta E_r = \frac{1}{2} P \delta u \qquad (1)$$

where P is the remote load, u is the imposed remote displacement.

For an increment of split growth, $d1$, the energy absorbed in forming new crack surfaces, dE_{ab}, is given by:

$$\delta E_{ab} = G_s t \delta 1 + G_d (1 \tan\alpha) \delta 1, \tag{2}$$

where G_s is the energy absorbed per unit area of split; G_d is the energy absorbed per unit area of delamination; t is the thickness of a 0° ply; and α is the delamination angle at the split tip.

Some of the global energy of the system is dissipated when the split extends with a corresponding increase in specimen compliance, dC,

$$\delta E_r = \tfrac{1}{2} P^2 \delta C. \tag{3}$$

For the damage zone to grow, $\delta E_r \geq \delta E_{ab}$,

$$\tfrac{1}{2} P^2 \delta C \geq G_s t \delta 1 + G_d 1 \delta 1 \tan\alpha \tag{4}$$

where P is the applied load on one quadrant only of the specimen given by

$$P = \sigma_\infty (W/2)(2t). \tag{5}$$

σ_∞ is the remote applied tensile stress on the rectangular tensile specimen, and W is the specimen width.

For the limiting case, $E_r = E_{ab}$,

$$\frac{1}{2}\frac{P^2}{t}\frac{\delta C}{\delta 1} = G_s + G_d \frac{1 \tan\alpha}{t} \tag{6}$$

(essentially, $G = G_c$).

G_c is the effective toughness of the laminate and G is the strain energy release rate. A 2-D finite element model determines $dC/d1$ numerically. For a range of split length between $1/a = 0$ and $1/a = 6$, it turns out (fortunately) that $dC/d1$ is constant, its value dependent on the angle α, the lay-up construction of the laminate and temperature.

Re-arranging Eqn. (6), the load for split initiation is given by

$$P_i = \left[\frac{2G_s t}{\delta C / \delta l_{l=0}}\right]^{1/2} \tag{7}$$

Quite simply, the value of G_s can be determined from a measurement of P_i. For subsequent split growth under monotonic loading;

$$l = \frac{P^2(\delta C / \delta l)}{2G_d \tan\alpha} - \frac{G_s}{G_d}\left[\frac{t}{\tan\alpha}\right]. \tag{8}$$

Dividing both sides of Eqn. (8) by notch length, a, and substituting for P (in terms of applied stress σ_∞), and dC/dl, [scaled from the finite element result $(\partial C / \partial l)|_{FE}$], this expression can be normalised as follows;

$$\frac{l}{a} = \frac{(\sigma_\infty)^2 (t)(W/2)_{FE}(2t)_{FE}}{G_d \tan\alpha (2a/W)} \left.\frac{\partial C}{\partial l}\right|_{FE} - \frac{G_s}{G_d}\left[\frac{t}{a\tan\alpha}\right], \tag{9}$$

where $\partial C / \partial l$ is the change in compliance of the FE model with split length; $(W)_{FE}$ is the width of FE model specimen; and $(t)_{FE}$ is the ply thickness in the FE model.

Provided $G_s < G_d$ (it turns out that it is), then the second term on the right-hand side of Eqn. (9) is small, and can be ignored:

$$\frac{l}{a} = \frac{(\sigma_\infty)^2 (t)(W/2)_{FE}(2t)_{FE}}{G_d \tan\alpha (2a/W)} \left.\frac{\partial C}{\partial l}\right|_{FE}. \tag{10}$$

Eqn. (10) indicates that for a given 2a/W, the ratio l/a is dependent only on applied stress, σ_∞. The normalised split length with applied stress curves for all $(90/0)_S$ specimens should be coincidental regardless of width. Eqn. (10) produces a good fit to data[1,2] using selected values of $a = 4°$, $G_d = 400\ J/m^2$ and $G_s = 160\ J/m^2$ for a carbon fibre-epoxy composite. (In similar experiments where epoxy was replaced with a matrix of polyetheretherketone (PEEK), $\alpha = 1°$, $G_d = 800\ J/m^2$ and $G_s = 400\ J/m^2$). The model can be extended to fatigue damage accumulation[1,2].

Incorporation of Residual Stress into the Finite Element Model

If thermal residual stresses are included in the model, then a simple compliance expression is no longer sufficient.

As the level of damage increases, three energy release contributions exist: (1) an increase in mesh-compliance caused by a change in the mechanical strain energy; (2) a relaxation of the residual stresses and hence a decrease in the thermal strain energy of the mesh; and (3) a small expansion of the mesh due to relieving of the residual stresses and therefore a work contribution from the applied load. The expression for the total potential energy released now becomes;

$$\partial E_r = \frac{1}{2}P^2\partial C - \partial E_{th} + P\partial v \tag{11}$$

E_{th} is the strain energy due to residual stresses only and v is the displacement of the top edge of the FE mesh before loading, measured from the position at $l/a = 0$. At a fixed temperature, the elastic properties are constant and E_{th} is proportional to the square of the remote residual stress. Similarly, displacement is caused by damage alleviating thermal contraction; therefore v is directly proportional to the temperature drop applied and to the magnitude of the residual stress. Incorporating the mechanisms of splitting and delamination:

$$\frac{1}{2}P^2\frac{\partial C}{\partial l} - \frac{\partial E_{th}}{\partial l} + P\frac{\partial v}{\partial l} = G_s t + G_d(\tan\alpha)l \tag{12}$$

The compliance change $\partial C/\partial l$ of the FE mesh is independent of split length. The functions of thermal strain energy $\partial E_{th}/\partial l$ and displacement $\partial v/\partial l$, however, are not independent of split length and can be described using linear functions of l/a. The rate of change of displacement is independent of specimen size for a constant 2a/W, but thermal strain energy has to be scaled from the FE result. Thus:

$$\frac{\partial E_{th}}{\partial l} = \frac{\partial E_{th}}{\partial l}_{FE}\left[\frac{Wt}{W_{FE}t_{FE}}\right] = \left[C_1 + C_2\left(\frac{1}{a}\right)\right]\left[\frac{Wt}{W_{FE}t_{FE}}\right] \tag{13}$$

$$\frac{\partial v}{\partial l} = \frac{\partial v}{\partial l_{FE}} = \left[C_3 + C_4\left(\frac{1}{a}\right)\right] \tag{14}$$

where C_1-C_4 are constants determined directly from finite element analysis for each temperature and material type. Substituting into Eqn. (12) gives:

$$\frac{1}{2}P^2\frac{\partial C}{\partial l}-\left[C_1+C_2\left(\frac{1}{a}\right)\right]\left[\frac{Wt}{W_{FE}t_{FE}}\right]+P\left[C_3+C_4\left(\frac{1}{a}\right)\right]=G_s t+G_d(\tan\alpha)l \qquad (15)$$

and hence:

$$l=\frac{\frac{1}{2}P^2(\partial C/\partial l)-G_s t-C_1 Wt/W_{FE}t_{FE}+PC_3}{(G_d\tan\alpha+C_2 Wt/aW_{FE}t_{FE}-PC_4/a)} \qquad (16)$$

If residual stresses are excluded from the analysis, C_1-C_4 are equal to zero and Eqn. (16) simplifies to:

$$l=\frac{\frac{1}{2}P^2(\partial C/\partial l)-G_s t}{G_d\tan\alpha} \qquad (17)$$

Substituting for P and $\partial C/\partial l$, and dividing both sides by the notch half-length, a , produces:

$$\frac{l}{a}=\frac{\frac{1}{2}\sigma_\infty^2 Wt(\partial C/\partial l)_{FE}W_{FE}t_{FE}-G_s t-C_1 Wt/W_{FE}t_{FE}+\sigma_\infty WtC_3}{(G_d\tan\alpha+C_2 Wt/W_{FE}t_{FE}-\sigma_\infty WtC_4)} \qquad (18)$$

Calculating G_S and G_d

Values of G_s can be determined from the stress to initiate damage, $\sigma_{\infty i}$, measured from x-ray radiography. At the onset of damage, the split length equals zero and Eqn. (18) can be rearranged to give:

$$G_s=\frac{\sigma_{\infty i}^2 W(\partial C/\partial l)_{FE}W_{FE}t_{FE}}{2}-\frac{C_1 W}{W_{FE}t_{FE}}+\sigma_{\infty i}WC_3 \qquad (19)$$

where substitution of appropriate values from finite element analysis gives the energy required for unit area of 0° ply splitting. The work of fracture for delamination, G_d, is calculated for a $(90/0)_s$ laminate at

each temperature by fitting Eqn. (18) to the experimental data for split growth. In some material systems the delamination angle increases with stress and a linear function of the form $N\sigma$ has to be substituted for α, where N was a constant determined for each temperature.

As the temperature is raised, the values of G_s and G_d generally increase. The greater ductility of the matrix increases its work of fracture and the energy required per unit area of new crack surface rises accordingly. The values of G_d differ in accordance with the toughness of the matrix materials.

The residual stress contribution is proportional to the delamination angle α; a thin delamination zone gives rise to stiff coupling between the 0° and 90° plies.

A Damage Model for Quasi-static and Post-fatigue Strength

Using a finite element representation of the damage at a notch tip, combined with the observed terminal damage-state and measured failure stress, the maximum tensile stress in the principal load bearing (0°) ply is approximately constant at laminate failure, regardless of the extent of damage[1,2]. This leads to a straightforward tensile stress failure criterion;

$$\sigma_{\infty f} = \frac{\sigma_{0f}}{K_t}, \tag{20}$$

where $\sigma_{\infty f}$ is the remote failure stress of the notched laminate; σ_{0f} is the localised tensile strength of the (0°) ply in the damage zone; and K_t is the terminal notch tip stress concentration factor. σ_{0f} is a material property which can be determined independently while K_t can be obtained from finite element modelling. For a centre-notched $(90/0)_s$ specimen K_t is;

$$K_t = \frac{6.3}{\left[1-(2a/W)^2\right](1/a)^{0.28}} = C_5\left[\frac{1}{a}\right]^{-0.28}. \tag{21}$$

Furthermore, the local strength of a 0° ply within the notch tip damage zone of a centre-notched tensile (CNT) specimen depends on the size of

the damaged zone (just like the strength of brittle solids depend on their volume);

$$\sigma_{0f} = \sigma_0 \left[\frac{V_0}{KV_{CNT}} \right]^{1/m}, \tag{22}$$

where σ_0, V_0 is a mean failure stress and reference volume. KV_{CNT} is the equivalent volume of the 0° ply in the notch tip damage zone; and m is the Weibull modulus.

The stress distribution at the notch tip varies with split length, l, and the delamination angle, α, at the tip of the split. In my experiments, $\alpha = 3.5°$, $K = 0.0014 + 0.0025\,(l/a)$; hence

$$\sigma_{0f} = \sigma_0 \left\{ \frac{V_0}{\left[0.0014 + 0.0025(l/a)8\left(a^2 t\right) \right]} \right\}^{1/m} \tag{23}$$

$$= C_6 \left\{ [0.0014 + 0.0025(l/a)]a^2 \right\}^{-1/m}. \tag{24}$$

$V_{CNT} = 8(a^2 t)$, where t is the thickness of the 0° ply.

Thermal strain mismatch between the 0° and 90° plies causes a state of residual compression parallel to the fibres in the load-bearing 0° ply. This reduces the maximum tensile stress and hence reduces K_t. As temperature is increased, K_t increases due to two mechanisms: (1) a reduction in the level of residual stress; and (2) a decrease in the lamina transverse and shear moduli. The latter causes an increase in the anisotropy of the specimen, forcing the 0° ply to carry a greater proportion of the applied load. If $\log(K_t)$ is plotted against $\log (l/a)$, straight lines can be fitted to the data for each temperature using the empirical function of the form:

$$K_t = \frac{C_5}{(l/a)^p} \tag{25}$$

where C_5 and p are constants.

Application to the CNT Specimen Notch Tip

The stress field at the tip of a notch in a CNT specimen can be determined by finite element analysis. To determine KV_{CNT}, the finite element results has to be scaled from a 2-layer quadrant to the dimensions of the actual specimen by defining a reference volume $V_{CNT} = 8a^2t_o$ (a is the notch half-length and t_o is half the total thickness of the 0° plies). K is obtained by integrating numerically using finite element results such that:

$$K \approx \frac{1}{a_{FE}^2}\left[\frac{1}{\sigma_{0p}}\right]^m \sum_{i=1}^{i=n} \sigma_i^m A_i \tag{26}$$

where σ_i is the stress at a single element integration point, A_i is the corresponding area associated with the integration point, n is the total number of integration points in the finite element mesh and σ_{0p} is the maximum stress in the distribution. KV_{CNT} therefore describes the equivalent volume of 0° ply in the CNT specimen that is subjected to the maximum stress σ_{0p}.

As split length increases, the stress gradients at the notch tip become less severe and a larger volume of material is subjected to a stress close to the peak stress. An increase in temperature results in a larger value of K due to the increasing size of the delamination zone. A larger angle α corresponds to more compliant shear coupling across the split and hence a larger equivalent volume.

In order to describe K as a function of $1/a$, empirical equations of the form:

$$K = C_6\left(\frac{1}{a}\right) \tag{27}$$

are fitted through the data, where C_6 is a constant.

If Eqn. (27) is inserted into Eqn. (22), the full expression for the strength of the 0° ply at each temperature becomes:

$$\sigma_{0f} = \sigma_o\left[\frac{V_o}{C_6(1/a)8a^2t_o}\right]^{1/m} \tag{28}$$

where σ_o, V_o and m are measured from Weibull experiments and C_6 is calculated using finite element results.

Notched Tensile Strength

As subcritical damage propagates from the notch tip, the stress concentration factor, K_t, continuously decreases (Eqn. (25)). Damage provides a progressive crack blunting mechanism and the peak stress in the 0° ply (σ_{0p}) is no longer proportional to the applied stress. The stress gradients near the notch tip are altered by a change in the stress distribution and as the splits grow, a larger volume of 0° ply is subjected to a stress near to the peak stress. This in turn, causes a reduction of the strength of the 0° ply (σ_{0f}) due to a Weibull dependence on the volume under stress (Eqn. (28)). Two competing mechanisms therefore exist as the splits extend – notch blunting and a reduction in 0° ply strength.

Application of the Tensile Failure Criterion

The remote stress on the notched specimen at failure is given by:

$$\sigma_{\infty f} = \sigma_o \left[\frac{V_o}{C_6 (1/a) 8 a^2 t_o} \right]^{1/m} \left[\frac{(1/a)^p}{C_5} \right] \tag{29}$$

The remote failure stress is a function of the damage state, characterised by $1/a$, at the point of failure. For typical values of p and m calculated previously, longer split lengths correspond to higher strength specimens. Equation (29) therefore requires an experimental measurement of the split length immediately prior to catastrophic failure to determine $\sigma_{\infty f}$.

For a $[90/0]_s$ lay-up, substituting for $1/a$ in Eqn (29) produces:

$$\sigma_{\infty f} = C_7 a^{-2/m} \left[\frac{\frac{1}{2}\sigma_{\infty f}^2 Wt (\partial C/\partial 1)_{FE} W_{FE} t_{FE} - G_s t - C_1 Wt / W_{FE} t_{FE} + \sigma_{\infty f} WtC_3}{(G_d a \tan\alpha + C_2 Wt / W_{FE} t_{FE} - \sigma_{\infty f} WtC_4)} \right]^{(p-1/m)} \tag{30}$$

where C_7 is a dimensional constant which must be determined for each temperature and material type. Eqn. (30) incorporates an implicit calculation of the damage state at failure and results in a remote strength prediction which is based entirely on independently determined parameters. The fracture energies, G_s and G_d, are calculated by curve fitting using the experimental data for damage growth, but no reference has been made to the data for tensile strength.

Conclusions

Once damage initiates, the stress distribution at the notch tip is altered by the growth of splits and delaminations and ultimate failure is controlled by the maximum notch tip stress in the load-bearing 0° plies, σ_{0p}. A damage-based model for notched tensile strength has been assembled, using the results of both finite element analysis and Weibull experiments. Thermal residual stresses are included into the model. Additional energy contributions are suggested that may arise due to interlaminar effects not included in the 2-dimensional finite element model.

References

1. Beaumont, P.W.R., Predictive Design and Certification Procedures: Modelling Fracture Stress, Fatigue Strength and Life-time of Composites and Structures. CUED/C-MATS/TR 241. First Report for EOARD (Special Contract Program SPC 98-4004), (January, 1998). Cambridge University Engineering Department, Cambridge, UK.

2. Beaumont, P.W.R., Towards a Predictive Design Methodology of Composite Laminate Patches Based on Physical Modelling of Failure Processes. Second Report for EOARD (Special Contract Program SPC 98-4004), February, 1998. Cambridge University Engineering Department, Cambridge, UK.